Simulation of HMA Compaction by using FEM

H.L. TER HUERNE†, M.F.A.M. VAN MAARSEVEEN†,

A.A.A. MOLENAAR‡ AND M.F.C. VAN DE VEN‡

†University of Twente, The Netherlands

‡Delft University of Technology, The Netherlands

This paper introduces a simulation tool for the compaction process of Hot Mix Asphalt (HMA) using a roller under varying external conditions. The focus is on the use of the Finite Element Model (FEM) with code DiekA, on its necessary requirements and on the presentation of simulation results. The approach requires the availability of a suitable material model, equipment to measure material parameters and a laboratory-testing program for fitting the correct material parameters. Subsequently, in discussing the simulation results attention is paid to; the principal stresses, strains and shear stresses inside the material during rolling, and the incremental displacements of the material. Furthermore, the simulated density path as a function of depth inside the layer is presented for a series of applied roller passes. In conclusion it can be stated that FEM approaches in general are well suited to simulate compaction processes of HMA on condition that the selected FEM comprises the right features.

Keywords: FEM Simulation; Asphalt pavement; Paving; Compaction; Critical State;

1 Introduction

It is difficult to construct a road with a homogeneous compaction level close to prescribed specifications. However, adequate compaction of Hot Mix Asphalt (HMA) applied in road construction is important for producing roads with good bearing capacity and a long life span. An extensive literature review on compaction of asphalt concrete has been done (Ter Huerne, 2004). One of the results of the study was that no fundamental tools for simulating the behaviour of compacting HMA currently exists. This research project aims to study the development of such a tool, as illustrated in figure 1. The following elements are crucial for the development of such a tool;

1. HMA material parameters
2. An HMA material model
3. A simulation tool
4. A compaction test section (for validation purposes)
5. Laboratory equipment (for deduction of the material parameters)

Unfortunately all these cannot be discussed in detail in one paper. Therefore the choice is made to discuss elements 1 to 4 briefly, but in enough detail to facilitate a more detailed discussion about the main issue of this paper; the results of a Finite Element Method (FEM) analyses applied to HMA compaction. Elements 1 to 4 will be discussed in paragraphs 2, 3 and 4. For more details about these elements the authors refer to ter Huerne (2004).

It is acknowledged that the results as presented here do not hold for all types of rollers, all type of material mixtures and all type of roller schemes. The approach must be seen as a first step in modelling HMA compaction. As such the rolling procedures are investigated, and, thereafter, the effects of static steel rolling on dense asphalt mixtures are investigated. If a model is available for simulating the rolling process it could be possible to undertake the rolling more efficiently with better end results. Improved, more homogeneous compaction, will lead to less maintenance.

The authors further acknowledge that: the compaction process of asphalt mixture is characterized by the material flow, in which the air voids are expelled and the material becomes compacted. In this simulation, the physical phenomenon is not truly studied. In the paper the material was assumed to be homogeneous. The compaction of materials is explained to be caused by plastic deformation.

2 Principles of Critical State Theory

The behaviour of compacted HMA used for roads, is normally characterised as viscous-elastic. Whilst studying the behaviour of the final compacted product viscous-elastic material models are in use (Di Benedetto, 1998). However, particularly when the mixture is hot and only partly compacted, or not compacted at all, plastic deformation is assumed to dominate the process indicating that it is better to characterise the material behaviour as elastic-plastic, see figure 2 (Figge, 1987). The plastic part of the material behaviour is caused by particle re-orientation. It is expected that at high temperatures, corresponding to low bitumen viscosities, hardly any cohesion will develop in the binder (see figure 2). This can also be found in Figge's thesis. (Figge, 1987). At lower temperatures, when cohesion

plays a role, it is necessary to introduce viscous-elastic behaviour. Below temperatures of 70°C, general cohesion becomes very important where in most cases the compaction process has already been finished.

In addition, several models describing particle re-orientation have been developed in soil mechanics. However for asphalt mixtures no constitutive models are available that describe the elastic-plastic behaviour during compaction. Ter Huerne (2004) makes the assumption that compaction of HMA is mainly caused by particle re-orientation and therefore it is possible to model the behaviour by using the Soil Mechanics' Critical State theory.

The critical state theory works with the stresses *p'* (isotropic normal compression stress) and *q* (deviatoric stress). For axial symmetrical situations, like a tri-axial test, these stresses can be calculated using the following equations;

$$p' = {}^{1}/_{3}\sigma'_{ax} + {}^{2}/_{3}\sigma'_{rad} \qquad (1)$$

$$q = \sigma_{ax} - \sigma_{rad} \qquad (2)$$

in which;

σ_{ax} = axial stress applied on the sample

σ_{rad} = radial stress applied on the sample

More details about these stress notations can be found in Atkinson (1993), Schofield and Wroth (1968) or Wood (1990).

One of the important aspects of that theory is the use of a yield locus. A yield locus gives a boundary between stress states that cause elastic (recoverable) deformations and plastic (irrecoverable) deformations. The critical state theory distinguishes between three stress situations when a material is deformed plastic. These situations are coupled to the

critical state stress situation, which implicitly is one of the situations itself. The *critical state situation* is defined as the ultimate condition of perfect plasticity in which plastic shearing can continue indefinitely without changes in volume of effective stresses (Wood, 1990). It is the highest level of q at $p' = p'_N$ (see figure 3). Furthermore, stress situations *on the dry-* and *wet-side* of critical state can exist. When the stress situation, as a result of plastic deformation is *on the wet side of critical state* (i.e. p' higher than $p'_{critical\ state}$,) the material tends to compact. The volume of the material decreases and the material becomes stronger. Due to the strength increase the yield locus increases too. The material can support the enforced stress combination and can even support larger loading stresses. Hence, the material behaviour is stable. When the stress situation as a result of plastic deformation is *on the dry side of the critical state* (i.e. p' lower than $p'_{critical\ state}$), the material tends to shear (figure 3). Initially the volume increases and the material become less compacted and less strong. Due to this, the yield locus, that represents the material strength, decreases as well. A material loaded to this condition (enforced stress level) behaves unstably. This is due to the decrease of strength i.e. the stress level stay equal whereas strength decreases. During this project the specific volume of the material is expressed in *VMA* (Voids in the Mineral Aggregate) although in soil mechanics it is usual to express this as the variable *v*. The relationship between *VMA* and *v* is interchangeable, if *VMA* is known *v* can be calculated and vice versa (if the material composition is known).

A particular amount of a granular material can have any volume. For every specific volume the material does have a particular yield locus (i.e. strength, see figure 4). Material in a loose state does have high *VMA* values and low strengths; materials in a dense

compacted state do have low *VMA* values and higher strengths. This theory appears to be quite suitable for modelling the mechanical behaviour of asphalt concrete mixtures.

The compaction simulations are done with the FEM code DiekA (Huétink 1986). Within this code the material model 'Rock' is available. In general this material model operates in accordance with critical state principles. Figure 3 illustrates the most important part of the Rock material model; the yield locus as the boundary between elastic and plastic stress situations. By using Rock, the shape of the yield locus is more or less fixed. Other critical state models use other shapes as can be seen in Van Eekelen and Van den Berg (1994), Schofield and Wroth (1968) and Vermeer (1980), although for compaction the most important part of the model (compaction cap, on the right side of P'_N) looks similar to other models. Additionally, the flow rule from Rock is always "associated" for the compaction zone of the model. This means that the direction of plastic flow (i.e. plastic shear deformation divided by the plastic volume deformation) is perpendicular to the direction of the yield locus at that particular stress point. During this project the main target was to check if FEM is suitable for doing HMA compaction simulations. In future projects we recommend examining the usefulness of developing models for a description of the mechanical behaviour of HMA during compaction. For example models that permit non-associated flow during compaction.

3 Developing Modified Hveem StabiloMeter

To quantify the HMA material parameters in accordance with the critical state theory and the Rock model one requires tri-axial testing equipment. In the compaction research project the Hveem StabiloMeter (HSM, Hveem and Davis, 1950) was selected for this purpose

because the HSM is a type of tri-axial test equipment. Like the triaxial cell, the HSM can measure material properties of axial symmetrical specimens. The most important advantage of the HSM is, that the radial pressure on the specimen is the result of the radial deformation of the material. That is very similar to the way radial stresses develop during compaction of material under field conditions. To enable the derivation of critical state parameters, the apparatus had to be modified (Ter Huerne, 2004), hence the Modified Hveem StabiloMeter (MHSM).

Inside the Stabilometer a test sample is surrounded by a rubber diaphragm and behind that diaphragm an air/oil mixture is enclosed inside the Stabilometer body. Loading a sample axially causes the radial sample deformation, which in turn increases the confining pressure on the sample. The air inside the oil/air mixture functions as a non-linear spring. By modifying the Stabilometer the airlock in the oil/air mixture is changed for a piston combined with a mechanical spring in a supplementary cylinder (figure 5). In this MHSM a radial deformation of the sample generates a displacement of the new involved piston. These piston displacements will change the confining pressure on the sample because of a change in the spring length. The radial confinement stress-strain relationship is adjustable by choosing different spring stiffness in the additional involved cylinder.

Due to the modification the sample confinement is approximately linear related to radial deformation of the sample. It is also possible to deduce the radial sample deformation because there is a known relationship between the radial sample deformation and the displacement of the piston. Another advantage of the modification is the improved volume control over the sample during the test. A test with the MHSM provides the primary ‘sample’ quantities:

- the axial loading force [kN],
- axial deformation [mm],
- radial stress [MPa], and,
- piston displacement of the HSM modification [mm].

From the radial and axial stresses and strains the soil mechanics quantities p', q and the strains ξ_{vol} and ξ_{sh} can be calculated. The *VMA* value (comparable to the specific volume value ν of a soil) of the sample can be calculated since the total volume of the sample and the amount of aggregate is known during every step. From this data the p'-q -*VMA* relation is derived during every instant of the test. During the test the *VMA* level decreases because of plastic flow or compaction.

4 Test programme and results

A laboratory-testing programme was set up for calibration of the material model parameters. The selected material was DAC 0/11, which meets the Dutch standard specifications (CROW 1995). The mixture is composed of: Norwegian granite stone fraction >2 mm, 75/25 % respectively of crushed/ natural sand, a combination of crushed limestone and fly ash filler, and a 80/100 Pen Bitumen. During normal HMA compaction processes the mixture cools from approximately 140°C to 70°C*. However, it was not possible to test at these temperatures with the MHSM. The compaction tests had to be done at room temperature of 20°C. To compensate for this mismatch in temperature, a viscosity

was chosen to simulate the various high temperatures in the test set-up. Special binders were used which have a comparable viscosity at 20°C to high compaction temperatures. In the test programme the following variables were varied:

- material temperatures (because of the change in viscosity at the test temperature of 20°C),
- confining stress-strain relationships,

The conceptual MHSM is equipped with (two) springs with different stiffness. It makes the variation of the confining stress-strain relationship possible on two levels. Testing materials at different temperatures is achieved by changing the bitumen viscosity. For that purpose the Shell laboratory manufactured three types of bitumen to simulate the viscosity of a 80/100 Pen bitumen at respectively 78, 94 and 141°C. The corresponding viscosities of the products at 20°C, being the test temperature were respectively 27, 5.6 and 0.34 PaS. In each test the following sample quantities *p'*, *q*, & *VMA* were calculated for every instant during the test, and the *p'*-*VMA* curves were plotted (figure 6). The path of the *log p'*-*VMA* curve firstly indicates the compactibility of the material. Secondly, it expresses how much pressure is needed to realise a specific volume decrease (at equal stress *q/p'* ratio). Comparing the paths of different material temperatures and mixture variations reveals the differences in compactibility between, for example, round and more angular materials.

From soil mechanics theory it is known that samples with a specific loading history do show bilinear loading lines when expressed in the *ln p'* - *VMA* plane. The material behaves elastic until a certain (re-loading) level after which it behaves elastic-plastic. This

---

* This is an estimate of the temperature of HMA during rolling, based on measurements done during construction of the compaction test section. The specific temperature of every constructed road section can vary widely and is a result

pattern is identifiable in the test results. Figure 6 shows the results of laboratory tests with respect to the elastic-plastic patterns as discussed. It also illustrates the lines of the reference mixture (78 °C), a surplus of round material and two hotter mixture temperatures (respectively 94 and 141 °C). The mixture with the surplus of round material is added to the test series as a reference because from practice and several compaction studies it is known that rounder material results in an easier compactable HMA mixture (Gauer, 1975).

Using the MHSM has fit the magnitude of the material parameters. The parameters were fitted for one material (a DAC 0/11) and two stress combinations. The effect of bitumen viscosity on measured material characteristics was not in line with road building expectations. The tests show that the lower the bitumen viscosity (the hotter the material) the more difficult it becomes to compact the mixture. It is not the main topic of this paper but the laboratory tests made quite clear that more research into the relationship between ‘bitumen viscosity’ and ‘mixture compactibility’ is recommended for future projects. More details about the results of the laboratory testing work can be found in Ter Huerne (2004).

At a certain stage during the compaction process of HMA, air voids inside the mixture become separated and can no longer be driven out of the material. Some simple calculations using the gas law of Boyle-Gay Lussac proposes that the extra stresses inside the mixture caused by this particular phenomenon are about 1.5 % related to the total stresses caused by rolling. It is assumed that it will not lead to large errors when this phenomenon is ignored. The simulations undertaken are 2 dimensional making use of plane stain stress assumption.

---

of mixing temperature and several other environmental factors.

5 Results of the FEM analyses

DiekA is the selected approach for doing the FEM calculations on compacting HMA. In mechanical engineering DiekA is used for simulating the rolling process of steel and therefore a cylindrical coordinate system is incorporated. Such a coordinate system is an advantage when modelling a rotating wheel or roller drum. By using the cylindrical coordinate system the local x-axis is defined along the arc of a circle, the z-axis is defined through the middle of roller drum. DiekA is a FEM approach that is able to do Arbitrary Lagrangian Eulerian (ALE) calculations. Such an approach is required for simulating material behaviour that keeps the middle between a solid (Lagrangian approach) and a liquid (Eulerian approach). ALE makes it possible that a material behaves partly as a fluid and partly as a solid; it can ‘stream in’ and ‘stream out’ of the finite element mesh. Contact elements are available in the approach. These elements enable modelling the contact surface of the roller drum and HMA material. Although DiekA fulfils most demands correctly it also has a shortcoming to overcome. Namely that currently it is not possible to enforce a roller drum ‘weight’ on the HMA as input into the simulation and to calculate the layer thickness reduction; one has to ‘operate’ the other way around: one has to pre-describe the layer thickness reduction and calculate the required rolling force. In conclusion it can be said that FEM approaches in general are suitable to simulate HMA compaction and they can therefore assist in increasing the knowledge of those processes. The research in this project further illustrated that it is possible to use DiekA for those simulations although it is possibly not the optimal approach. If load controlled calculations are possible this would greatly help to simplify the simulation process.

Figure 7 illustrates the differences between “reality” and the “simulated” situation. This paper focuses on the results of a.) a single roller pass, and b.) six successive roller passes in terms of *VMA* and bulk density, elastic and plastic deformation, contact stiffness and stress.

5.1 Simulation of a single roller pass

Essential output for a single roller pass simulation is:

- vertical roller force,
- the shape of the curve represents the top of the HMA surface during compaction from upstream to downstream of the roller drum,
- deformation pattern (volumetric strain and deviatoric strain) in the vertical direction after rolling, isotropic normal compression stress pattern *p’*, and the deviatoric stress pattern *q*,
- shear stress σ_{xy},
- the way the material moves through the mesh (i.e. analysing the particle tracing positions),
- incremental displacements in the x and y planes (i.e. horizontal and vertical directions).

Subsequently the most important items will be discussed separately.

5.1.1 The free HMA material surface. Figure 8 shows the free material surface and the roller drum outline (perimeter) for a specific simulated roller pass from the test section experiment.

The figure illustrates that the roller drum penetrates the HMA material. This cannot be true in reality. Penetration (also called overlap) of the two interfaces of a contact element is a well-known phenomenon in FEM simulations. The extent of overlap depends on the contact stiffness in the normal direction. Contact parameters must be quantified in such a way that they approximate real behaviour. It is allowable that the estimated contact parameters contain small errors. When the simulation set-up is well designed; a minor variation of the contact parameters will not disrupt the integrity of the results. The way the upper material surface flows (more or less smoothly), forms a check on the tuning of the contact stiffness to the material stiffness being modelled. The material stiffness changes as a result of each subsequent roller pass. The contact stiffness parameters should be adjusted to reflect the increasing material stiffness. Contact stiffness in between 2.0 and 20.0 MPa gave good results in smooth-running simulations from the early roller passes until later passes on the more compacted material. The applied contact stiffness also determines the extent of overlap during the simulations: the overlap was between 0.2 and 1.0 mm. The overlap of 1.0 mm equals about 30% of the upper elements thickness (e.g. 3.5 mm). Such an overlap is quite acceptable in relation to the prototype character of the calculations. The main problem with overlap is that it affects the geometry of the roller drum.

Another element that can be extracted from the figure is the material recovery behind the roller drum. The extent of this recovery depends on the stress level that is obtained by rolling in combination with the recoverable material properties (i.e. the linear

elastic parameters E and ν used by Rock). The maximum stresses are not known prior to the simulations and thus the extent of recovery must be estimated; after all, the layer thickness reduction was a prescribed variable during the simulation. The roller drum must (vertically) be positioned at such a level that with respect to overlap and material recovery the layer thickness reduction should be as desired.

5.1.2 Principal stresses and strains in the material. By means of the FEM DiekA the four strain components are computed for every node*; the elastic shear strain, ε_{sh_el}, the plastic shear strain, ε_{sh_pl}, the elastic volumetric strain, ε_{vol_el} and the plastic volumetric strain, ε_{vol_pl}. The strains of most interest are the plastic ones (ε_{vol_pl} and ε_{sh_pl}). The first one, ε_{vol_pl}, because it represents the irrecoverable volumetric strain, which equals the compaction progression. The second one, ε_{sh_pl}, because it is plausible that there is a relationship with shearing of the material and the risk of the occurrence of roller fissures. Irrecoverable strains are caused by the stress situation inside the material related to the yield locus (i.e. the limit where elastic (recoverable) is turning into plastic (irrecoverable)).

Figure 9 shows the stress paths that points inside rolled material follow at a specific depth. The results at four depths (y = 0.0, 37.6, 52.3 and 55.8 mm) are illustrated in the p' and q space. In figure three (parts of) yield loci are plotted to indicate where the stress path meets the yield locus. From the figure the stress level at which the material starts to flow plastic can be analysed.

5.1.3 Shear stresses. Shear stresses are responsible for shearing of the material. In figure 10 the shear stress pattern of roller pass 05 is illustrated. Intuitively, these shear stress patterns give an excellent view on what really occurs inside the material when a roller is compacting it. The shear strain pattern shows the reverse of the shear stresses beneath the roller drum. Just in front of the roller drum the material is pushed up (initially square material elements would become high and small). Under and behind the roller drum centre the material becomes squeezed horizontally (initially square material elements would become wide and thin). The largest rate (change) in shear stress occurs under the roller drum just in front of its centre. In this context it is also interesting to consider the rotation of the principal stresses inside the material during rolling (figure 11). In the figure the length of the vectors represents the local stress levels.

5.1.4 Incremental displacements x and y. Figure 12 illustrates the incremental displacements (i.e. displacement per pre-described deformation step) of the material under compaction in the horizontal direction. Areas with a negative sign express displacement in the rolling direction, areas with a positive sign displacement opposite to the rolling direction. The pre-described incremental displacement is the relative displacement of the material related to the roller drum. When a roller drum drives at a certain speed it rides a particular distance in a unit of time. Every deformation step of the material can also be seen as a fixed time unit. Therefore the displacement of the material per step size can be linked

---

* More in detail the stresses and strains will be calculated in the Gauss point of the elements. From the Gauss point stresses and strains will be extrapolated to the nodal points of the elements. The output of the calculation will then present an averaged value of the stress and strain over all elements involved.

to the speed of the roller. This argument not only holds for the horizontal displacements and speed, but also for the vertical material displacements, hence, the vertical material deformation rates can be analysed from the DiekA results.

The dark area (figure 12) directly beneath the contact surface roller drum-rolled material indicates material displacement up to 0.002 mm in the direction of rolling. The material is enforced underneath the roller drum with 0.2 mm per step so the local horizontal material displacement rate in the dark area is up to 1% of the roller speed. The lighter areas indicate a material displacement of 0.0007 mm per step, opposite to the direction of rolling. This is about 0.35% of the roller speed (in the opposite direction). Also at the top of the layer just in front of and just behind the roller drum material displacement is opposite to the rolling direction. Apparently the material seems to be restrained (or obstructed) by the roller drum.

The bulk of the material has a speed around zero, whereas locally small areas exist where the speed is opposite to the direction of rolling. Intuitively such a pattern is plausible. When at certain locations the speed is below the average then it must be higher at other areas because at the borders the speed of the ‘inflow’ and ‘outflow’ is pre-described on the average level of 0.2 mm/step.

5.2 Simulation of multiple roller passes

Thus far it has been shown that an analysis of the results of a single roller pass yields loads of information. Nevertheless, a typical roller pass forms part of an overall rolling process, that requires 10 to 15 passes. The first passes are of major importance and also the most

critical in realising good compaction without generating damage. When simulating a subsequent roller pass, the results from previous roller passes, in terms of material compaction state, must be taken into account.

An item of major interest in a rolling process is the progress of compaction in the vertical direction of the layer. Figure 13 show the progress in bulk density as calculated by means of DiekA during 6 simulated roller passes applied on a specific road section. The progress (increase) of the bulk density is of course equal to the progress (decrease) of the Voids in the Mineral Aggregate (*VMA*, not shown here).

Analysis of the progress in compaction, with respect to the height of the material in the layer, shows that the first 6 roller drum passes (first three roller passes) is the most important. During these passes the bulk density increased from about 2070 to 2220 kg/m^3. Figure 14 shows (a) the depths inside the layer where maximum compaction progression is achieved, and (b) the extent of maximum compaction progression per pass. The figure shows that the first roller drum pass achieves the largest compaction progress in the top region of the layer. In the second roller drum pass the largest compaction progress occurred low in the layer whereas medium compaction progress is achieved high in the layer. During the third roller drum pass the majority of the compaction increase is achieved in the middle of the layer. This seems to be a process of levelling. Large compaction increase is achieved at positions where the stresses are high (first pass high in the layer) and the current material is ‘soft’ (because of compaction already achieved, e.g. pass 2 ‘low’), or a combination of these two (pass 3 ‘middle’).

Analysis of the compaction progress shows that, a more homogeneously compacted layer was achieved later on (after about 6 passes) probably because of the nature of this

levelling process. Also, the compaction progress per roller step decreases as the rolling process proceeds. This was also measured while monitoring a constructed experimental test section. The simulations indicate that the highest compaction level is achieved at a depth of about 38 mm from the bottom of the layer after the 6 roller passes were applied

6 Conclusions

Due to the analogy between HMA and granular materials it should be possible to adopt the critical state theory to model the behaviour of particle-based materials like HMA during compaction. The theory operates with a yield locus as a boundary between plastic and elastic stress situations. Yield loci and *VMA* levels can grow or shrink due to achieved loading stress combinations.

After modifying the Hveem Stabilometer it proved to be suitable to deduce critical state parameters. The material characterisation is achieved for one material (a DAC 0/11) at three ‘temperatures’ (i.e. three bitumen viscosities). Unexpected was the fact that a softer bitumen led to harder compactable mixtures.

With use of FEM it is possible to simulate and study the progress of HMA compaction in detail. FEM simulations offer insight into what actually happens during compaction within the material. However, the FEM tool used must be suitable for the task. In the case of rolling HMA, the selected approach should be of the ALE type, it must be able to model contact and the approach must contain a material model that is suitable to describe HMA material behaviour during compaction.

For this research project the FEM code DiekA was selected. DiekA can do ALE calculations and can model contact phenomena. Inside DiekA the material model “Rock” is

available, a model that in general operates in accordance with critical state principles. With some adaptations it is possible to run simulations of HMA mixtures being compacted using a static steel roller. Good insight into stress, strain and deformation patterns could be obtained although an appropriate roller drum weight could not be calculated. ALE is a prerequisite for simulation of rolling processes; it lets material flow through the mesh, and it is required for outlining contact elements. A rolling process cannot be simulated without contact. The ALE method handled the outlining of nodes perfectly on both sides of contact elements.

In conclusion it can be stated that FEM approaches in general can be used to simulate the compaction processes of HMA on condition that the selected FEM comprises the right features. The simulations did improve the insight in stresses, strains and material displacements caused by rolling. However, a skilled operator is required to undertake the simulations. An improved HMA compaction material model should be developed for calculation of the correct rolling forces.

References

Atkinson, J., The Mechanics of Soils and Foundations, McGraw-Hill, London, 1993.

Di Benedetto, H. and Ch. de La Roche., State of the Art on Stiffness Modulus and Fatigue of Bituminous Mixtures. In *Bituminous Binders and Mixes*, L. Francken, Spon, London (UK). RILEM Report 17, 1998, pp. 135-180.

C.R.O.W., Standaard RAW Bepalingen 1995. C.R.O.W, Ede, 1995.

Figge, H., Verdichtungs- und Belastungsverhalten Bituminöser Gemische. PhD thesis, Technische Hochschule Aachen, 1987.

Hveem, F.N. and H.E. Davis, Some concepts concerning triaxial compression testing of asphaltic paving mixtures and subgrade materials. *A compilation of papers Presented at the First Pacific Area National Meeting, San Francisco, 10 October 1949 and Fifty-Third Annual Meeting,* Atlantic City 28 June, 1950. ASTM, Philadelphia (USA), 1950, pp. 25-54

Huétink, J., On the simulation of thermo-mechanical forming processes. PhD thesis, Twente University, Enschede, 1986.

Gauer, P.K., Eine Analyse der Verdichtungswilligkeit und des Verformungswiderstandes von bituminösem Mischgut bei Verdichtung im Gyrator. Ph.D. thesis, Technische Hochschule Darmstadt, 1975.

Schofield, A. and Wroth, P., Critical state soil mechanics, London, 1968.

Ter Huerne, H.L., A Simulation Tool for Compaction of HMA using Critical State Principles, PhD thesis, Twente University, Enschede, 2004.

Ter Huerne, H.L., M.F.C. van de Ven, A.A.A. Molenaar, M.F.A.M. van Maarseveen, Using critical state theory and Modified Hveem StabiloMeter for modelling asphalt material behaviour. In *Proceedings ICCES'04 conference*, Madeira, Portugal, 2004.

Van Eekelen, S.J.M. and P. Van den Berg,. The Delfst Egg model, a constitutive model for Clay. In *DIANA Computational mechanics proceedings '94*, Kluwer, Dordrecht, 1994, pp 103-116.

Vermeer, P.A., Formulation and analysis of sand deformation problems. Ph.D. thesis, Delft University of Technology, Delft, 1980.

Wood, D.M., Soil Behaviour and Critical State Soil Mechanics, Cambridge University Press, 1990.

List of figures (captions)

Figure 1. Overview of the research project; the paper focuses on the shaded area.

Figure 2. Rheological behaviour of HMA during compaction, elastic – plastic – viscous, (Figge, 1987).

Figure 3. The shape of the yield locus of the used "Rock" material model.

Figure 4. Four yield loci for a material as a result of different compacted states and two elastic – plastic stress paths plotted in the *p'-q-VMA* space (Ter Huerne, 2004).

Figure 5. The principles of the Modified Hveem StabiloMeter, (ter Huerne, 2004).

Figure 6. The mean *log p'-VMA* curves of the different temperature mixtures and the low bitumen content.

Figure 7. The similarities and differences of a real rolling process (left) on a HMA material compared to a simulation of it by using FEM (right).

Figure 8. The free upper material surface of the HMA and the outline of a first roller pass on fresh material.

Figure 9. Stresses at four depth levels expressed in the *p':q* plane together with three (partial) yield loci.

Figure 10. Shear stresses as a result of a first roller pass on fresh material.

Figure 11. The principal stresses in the HMA material during rolling.

Figure 12. Incremental material displacements in the x direction (i.e. horizontal material displacement). A negative sign means displacement in the rolling direction, a positive sign means displacement opposite to the rolling direction.

Figure 13. Development of the bulk density of the material achieved by multiple roller passes.

Figure 14. Position inside the HMA layer (depth) where maximum compaction progression occurs (a) and the maximum achieved compaction progression in kg/m^3 per applied roller pass (b).

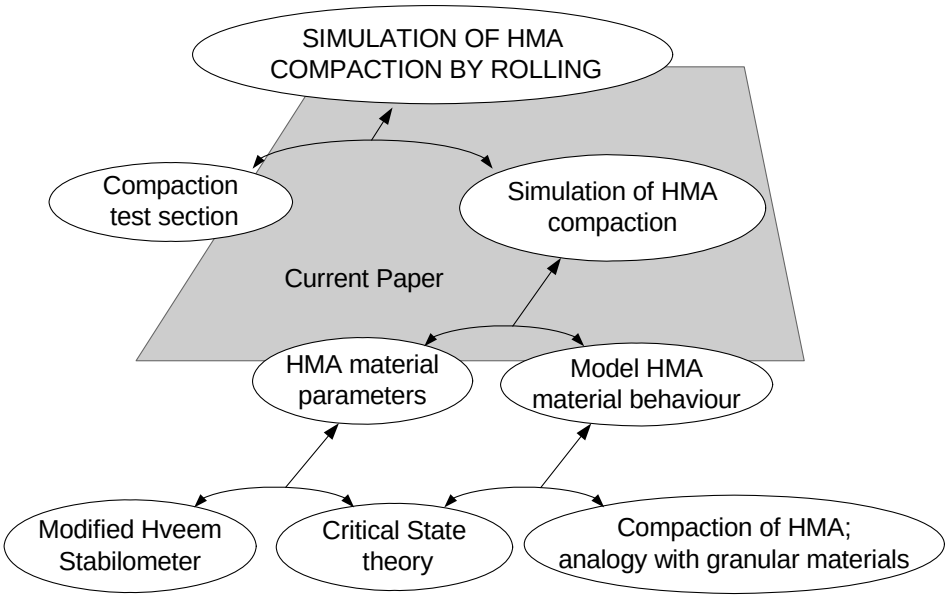
SIMULATION OF HMA COMPACTION BY ROLLING
Compaction test section
Simulation of HMA compaction
Current Paper
HMA material parameters
Model HMA material behaviour
Modified Hveem Stabilometer
Critical State theory
Compaction of HMA; analogy with granular materials

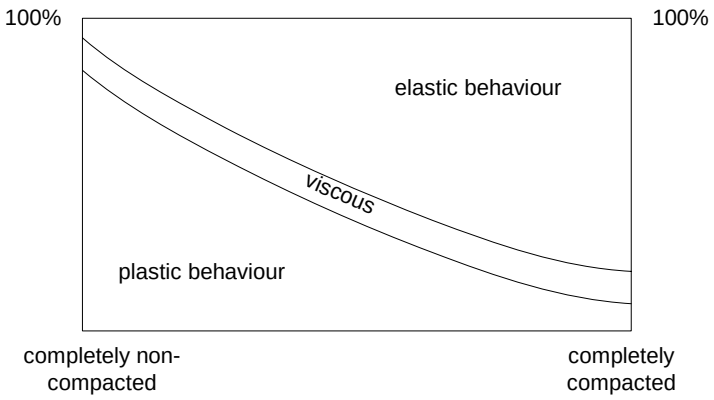
100%
100%
elastic behaviour
viscous
plastic behaviour
completely non-compacted
completely compacted

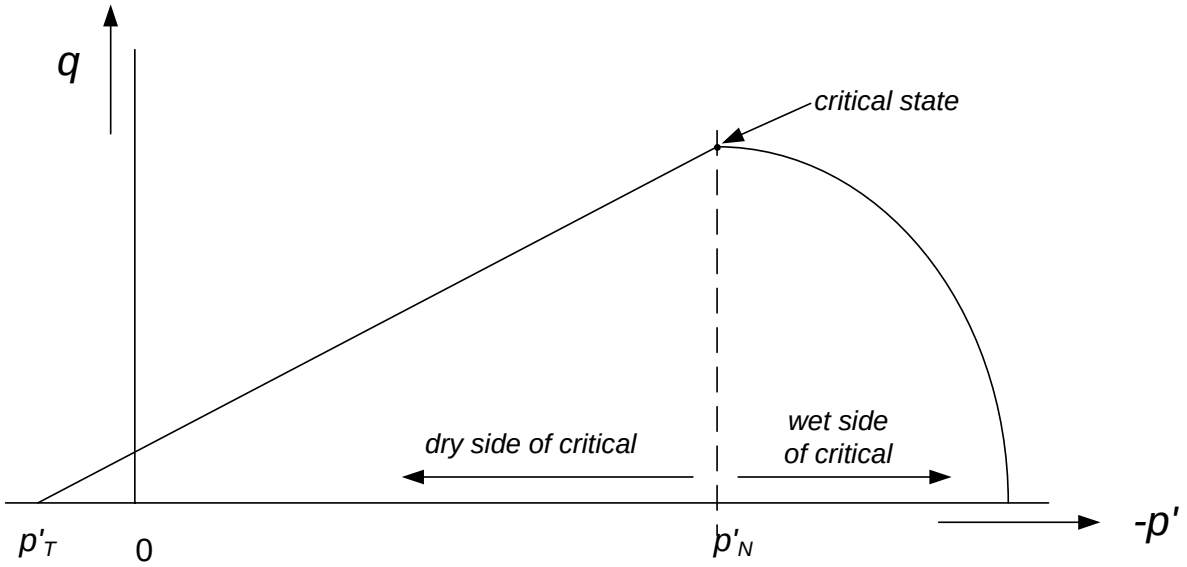
q
critical state
dry side of critical
wet side
of critical
p'T
0
p'N
-p'

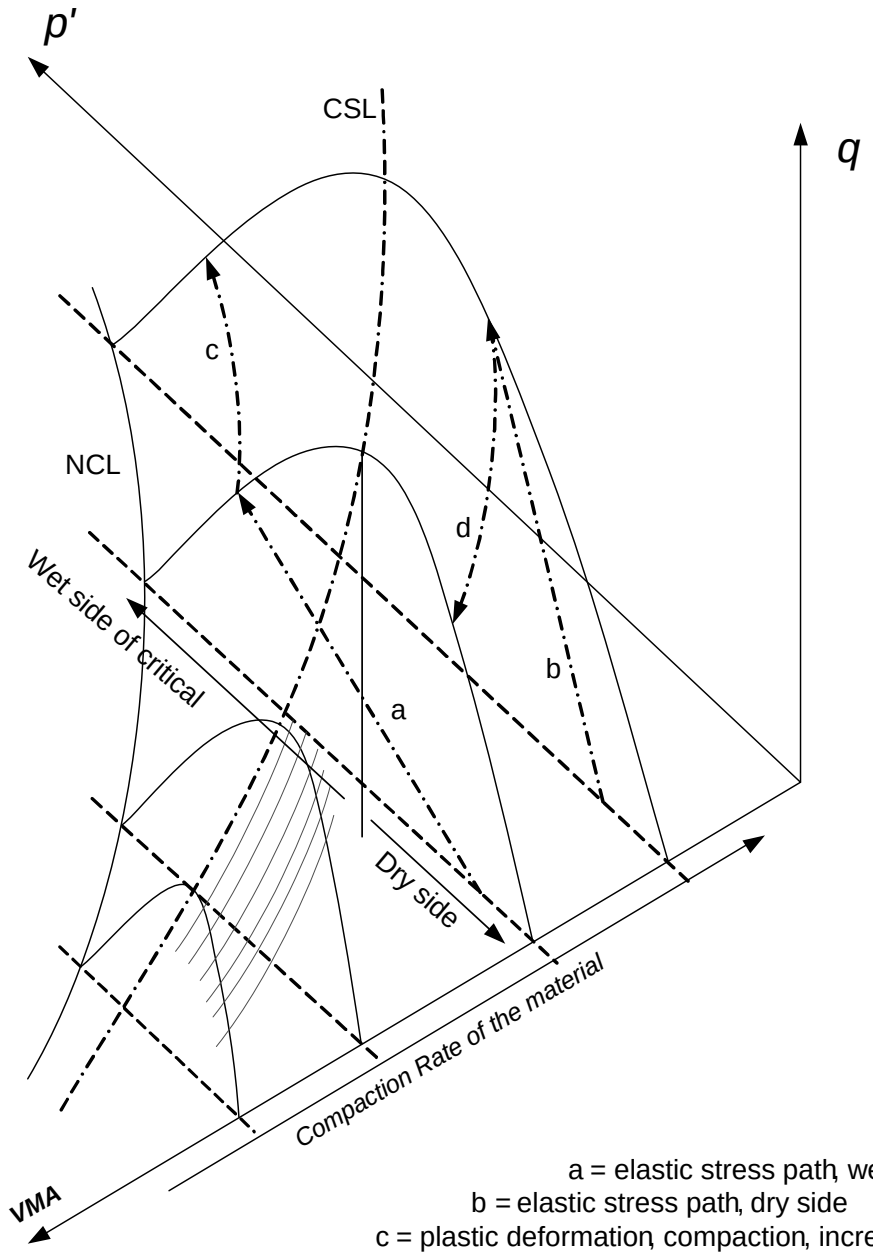

a = elastic stress path, wet side
b = elastic stress path, dry side
c = plastic deformation, compaction, increase yield locus
d = plastic deformation, shear, decrease yield locus

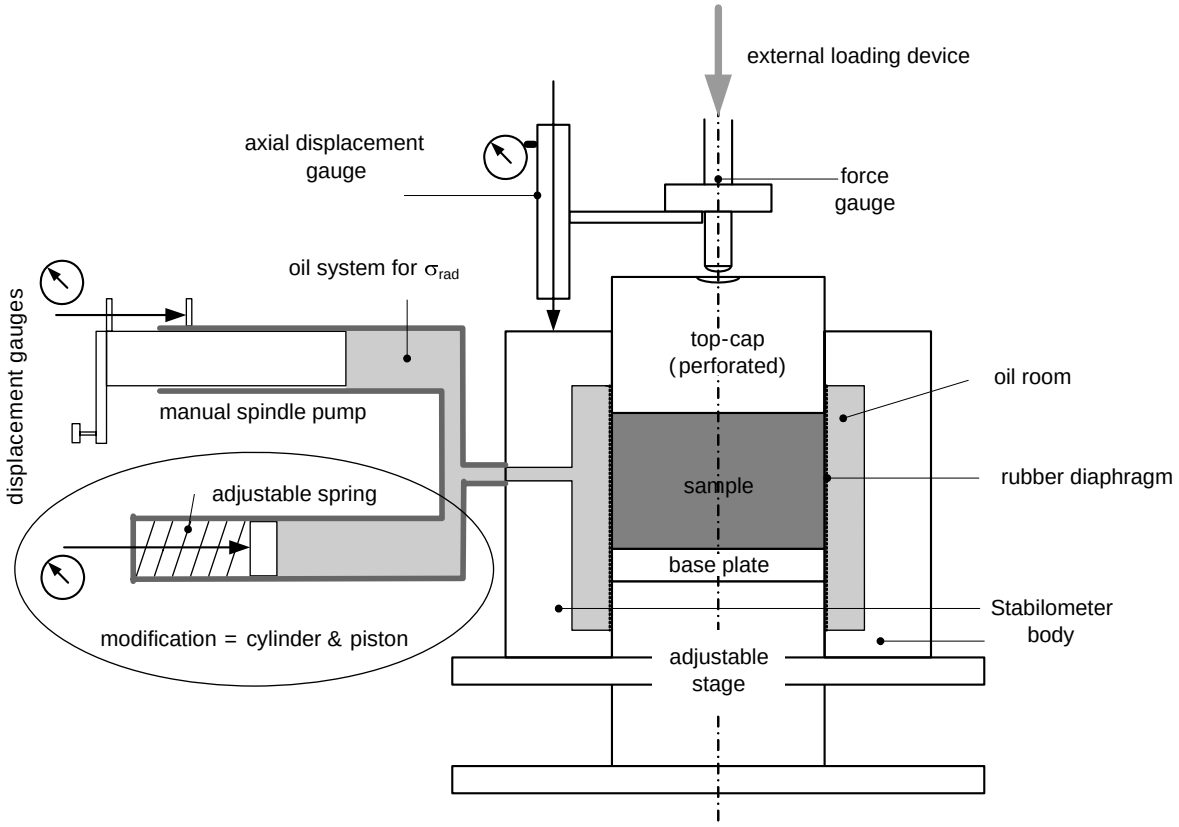
external loading device
axial displacement gauge
force gauge
oil system for σ_{rad}
displacement gauges
top-cap (perforated)
oil room
manual spindle pump
sample
rubber diaphragm
adjustable spring
base plate
Stabilometer body
modification = cylinder & piston
adjustable stage

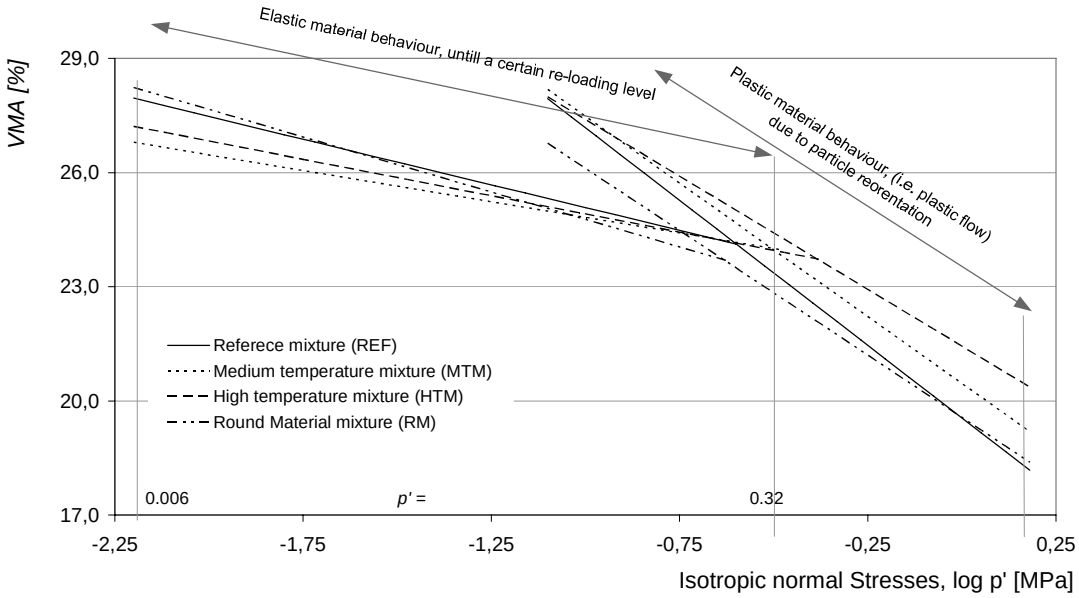
Elastic material behaviour, untill a certain re-loading level
Plastic material behaviour, (i.e. plastic flow) due to particle reorientation
VMA [%]
29,0
26,0
23,0
20,0
17,0
Referece mixture (REF)
Medium temperature mixture (MTM)
High temperature mixture (HTM)
Round Material mixture (RM)
0.006
p' =
0.32
-2,25
-1,75
-1,25
-0,75
-0,25
0,25
Isotropic normal Stresses, log p' [MPa]

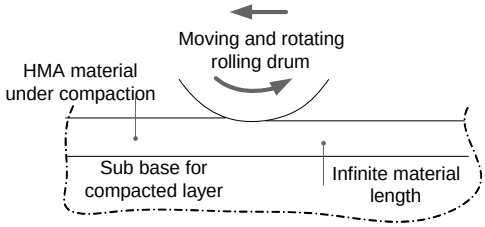

Reality

Load is fixed, displacement is the result

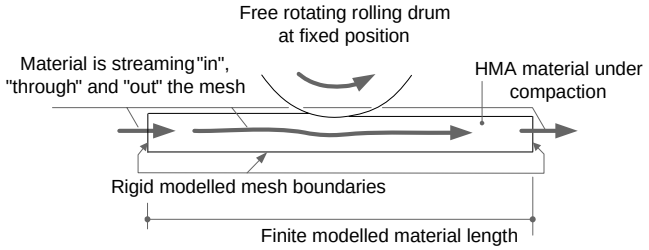

Simulation

Displacement level is pre-described, loading force is the result

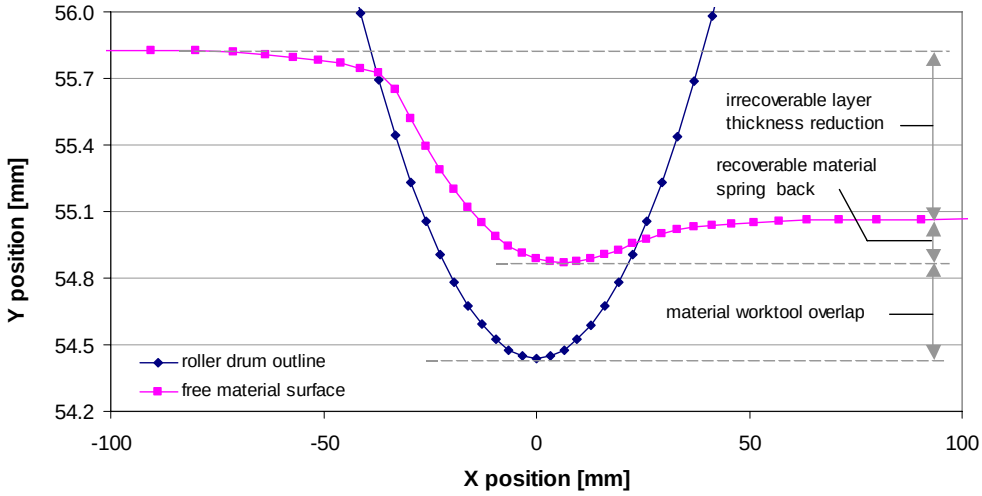
56.0
55.7
55.4
55.1
54.8
54.5
54.2
Y position [mm]
-100
-50
0
50
100
X position [mm]
irrecoverable layer
thickness reduction
recoverable material
spring back
material worktool overlap
roller drum outline
free material surface

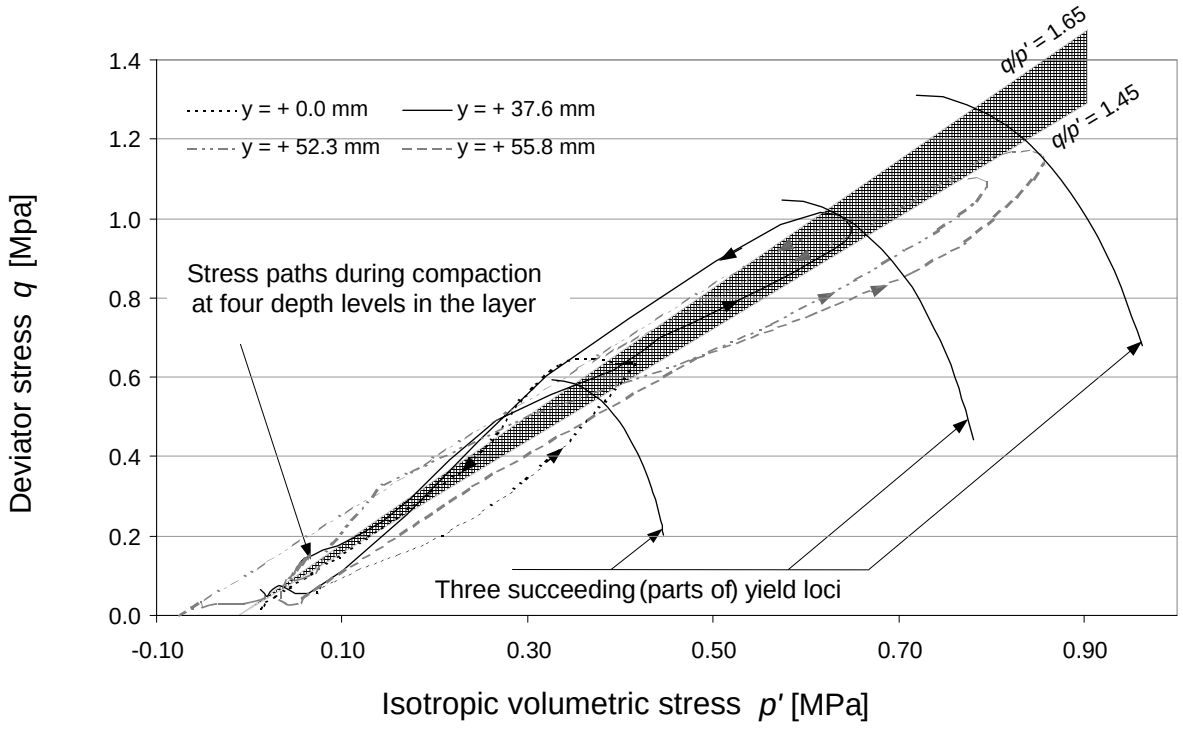
1.4
1.2
1.0
0.8
0.6
0.4
0.2
0.0
-0.10
0.10
0.30
0.50
0.70
0.90
Deviator stress q [Mpa]
Isotropic volumetric stress p' [MPa]
y = + 0.0 mm
y = + 37.6 mm
y = + 52.3 mm
y = + 55.8 mm
q/p' = 1.65
q/p' = 1.45
Stress paths during compaction
at four depth levels in the layer
Three succeeding (parts of) yield loci

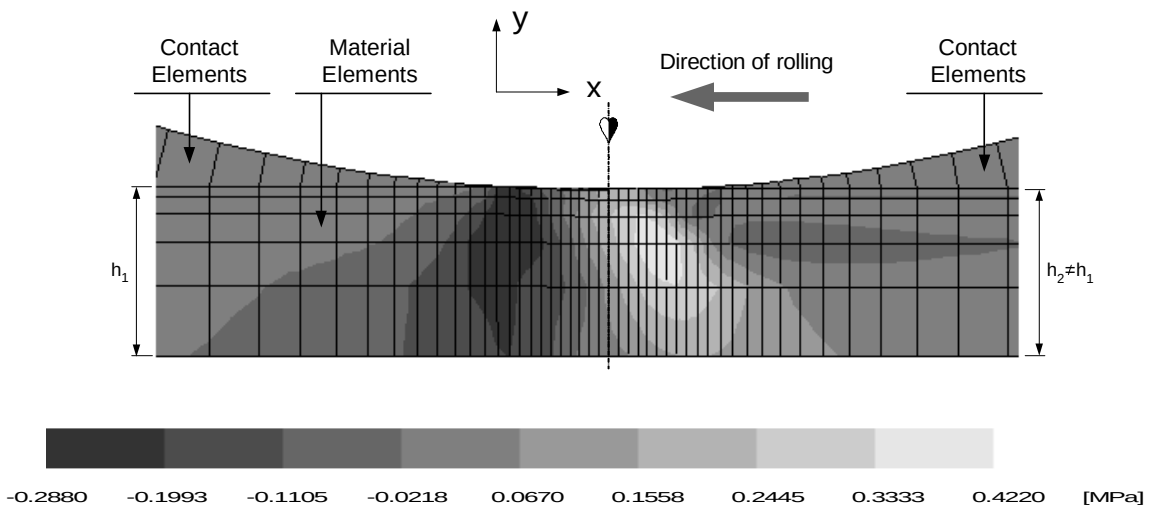
y
x
Contact Elements
Material Elements
Direction of rolling
Contact Elements
h1
h2≠h1
-0.2880
-0.1993
-0.1105
-0.0218
0.0670
0.1558
0.2445
0.3333
0.4220
[MPa]

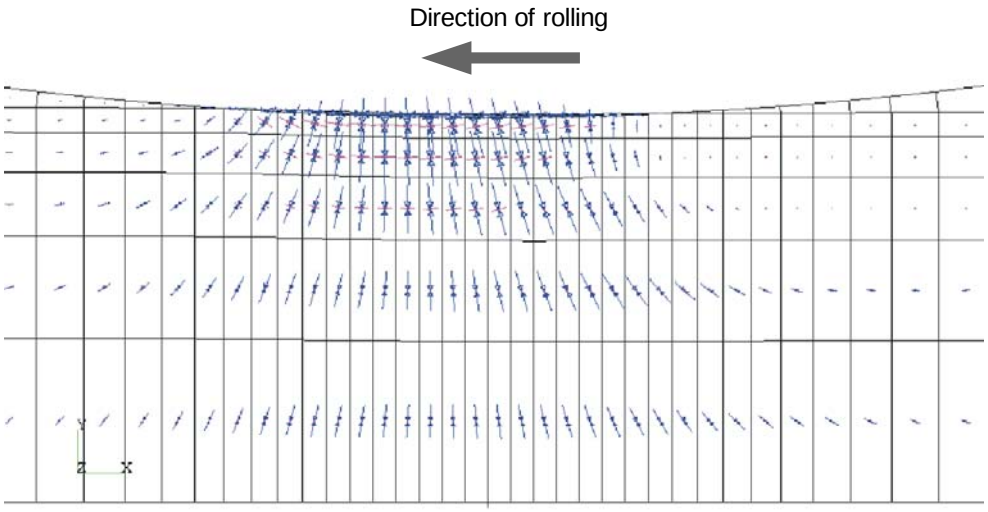
Direction of rolling

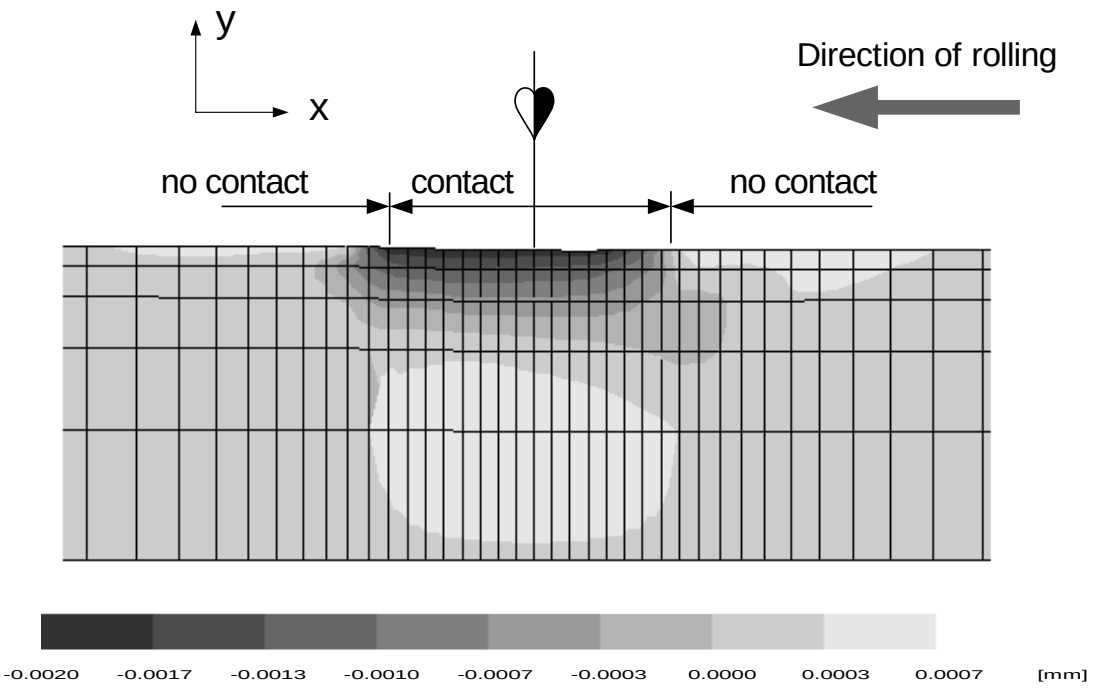
y
x
Direction of rolling
no contact
contact
no contact
-0.0020
-0.0017
-0.0013
-0.0010
-0.0007
-0.0003
0.0000
0.0003
0.0007
[mm]

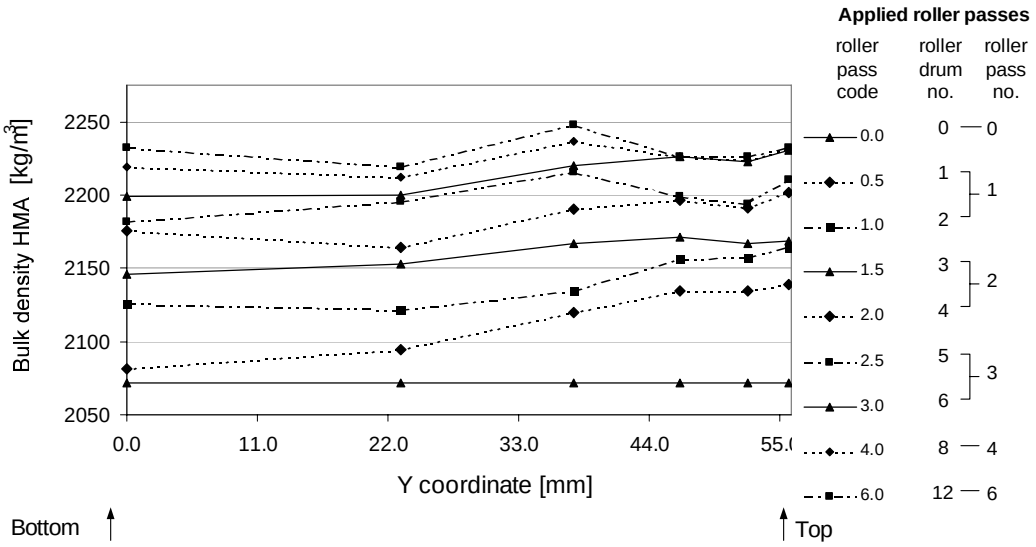
Applied roller passes
roller pass code
roller drum no.
roller pass no.
Bulk density HMA [kg/m³]
2250
2200
2150
2100
2050
0.0
11.0
22.0
33.0
44.0
55.0
Y coordinate [mm]
0.0
0.5
1.0
1.5
2.0
2.5
3.0
4.0
6.0
0
1
2
3
4
5
6
8
12
0
1
2
3
4
6
Bottom
Top

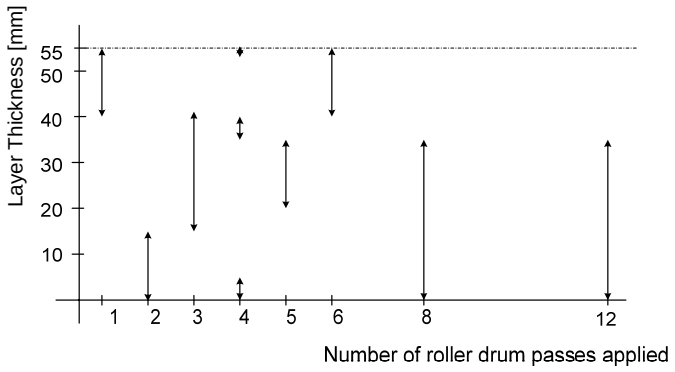
Layer Thickness [mm]
55
50
40
30
20
10
1
2
3
4
5
6
8
12
Number of roller drum passes applied

(a)

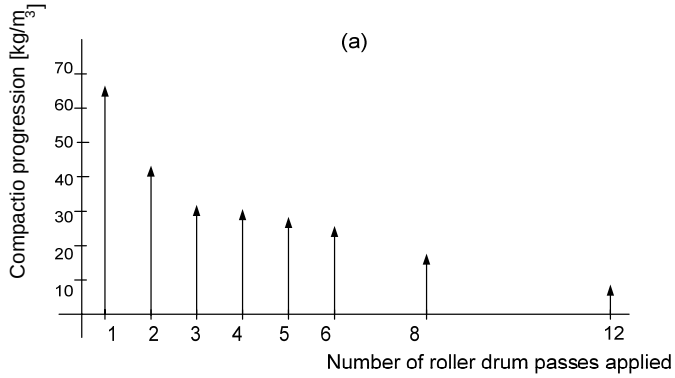
Compactio progression [kg/m3]
70
60
50
40
30
20
10
1
2
3
4
5
6
8
12
Number of roller drum passes applied

(b)